JOC The Journal of Organic Chemistry

pubs.acs.org/joc Article

Practical Remdesivir Synthesis through One-Pot Organocatalyzed Asymmetric (*S*)-P-Phosphoramidation

Veeranjaneyulu Gannedi, Bharath Kumar Villuri, Sivakumar N. Reddy, Chiao-Chu Ku, Chi-Huey Wong,* and Shang-Cheng Hung*

Cite This: *J. Org. Chem.* 2021, 86, 4977−4985 Read Online

ACCESS | Metrics & More | Article Recommendations | Supporting Information

ABSTRACT: Remdesivir, an inhibitor of RNA-dependent RNA polymerase developed by Gilead Sciences, has been used for the treatment of COVID-19. The synthesis of remdesivir is, however, challenging, and the overall cost is relatively high. Particularly, the stereoselective assembly of the P-chirogenic center requires recrystallization of a 1:1 isomeric *p*-nitrophenylphosphoramidate mixture several times to obtain the desired diastereoisomer (39%) for further coupling with the D-ribose-derived 5-alcohol. To address this problem, a variety of chiral bicyclic imidazoles were synthesized as organocatalysts for stereoselective (*S*)-P-phosphoramidation employing a 1:1 diastereomeric mixture of phosphoramidoyl chloridates as the coupling reagent to avoid a waste of the other diastereomer. Through a systematic study of different catalysts at different temperatures and concentrations, a mixture of the (*S*)- and (*R*)-P-phosphoramidates was obtained in 97% yield with a 96.1/3.9 ratio when 20 mol % of the chiral imidazole-cinnamaldehyde-derived carbamate was utilized in the reaction at −20 °C. A 10-g scale one-pot synthesis via a combination of (*S*)-P-phosphoramidation and protecting group removal followed by one-step recrystallization gave remdesivir in 70% yield and 99.3/0.7 d.r. The organocatalyst was recovered in 83% yield for reuse, and similar results were obtained. This one-pot process offers an excellent opportunity for industrial production of remdesivir.

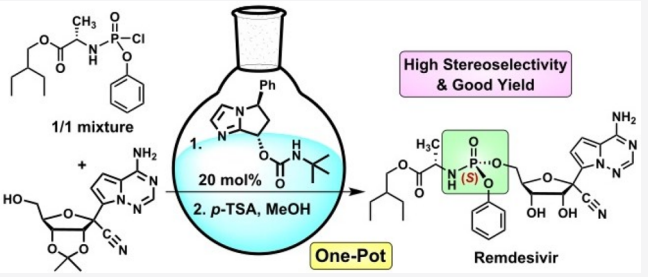

INTRODUCTION

The respiratory disease COVID-19 caused by the severe acute respiratory syndrome coronavirus 2 (SARS-CoV-2) is currently the most severe global health catastrophe of the century.[1−3] SARS-CoV-2 consists of four structural proteins: spike (S), nucleocapsid (N), envelope (E), and membrane (M) proteins, which play significant roles in virus maturation and infection.[4] The S-proteins are richly glycosylated and are presented as a trimer on the viral surface with a characteristic bulging appearance[5] for interaction with human angiotensin-converting enzyme 2 (ACE2) receptor on airway epithelial cells during the initial step of infection.[6−9] Further cleavage of the S-proteins by human transmembrane protease serine 2 (TMPRSS2) initiates the viral fusion and endocytosis process.[10] Once the RNA genome is released, it hijacks the cell machinery and translates into polyprotein 1a (PP1a) and polyprotein 1ab (PP1ab), which are subsequently cleaved by viral 3C-like (3CL) and papain-like (PL) proteases to generate 16 nonstructural proteins (NSP) as a replication-transcription complex (RTC).[11] Replication of the viral RNA by the RNA-dependent RNA-polymerase (RdRp, NSP12)[12] and transcription of the viral RNA into mRNA by RTC enable the next translational process to produce the S-, N-, E-, and M-proteins as well as others.[13] Post-translational modifications such as glycosylation followed by assembly of all components form viral vesicles for transport and release.[14,15]

Remdesivir **1** (GS-5735, Figure 1) is a broad-spectrum antiviral compound that was developed by Gilead Sciences for the treatment of hepatitis C and Ebola virus infections.[16,17] The phase III clinical trials of the drug, conducted in The Democratic Republic of Congo, showed insignificant effect

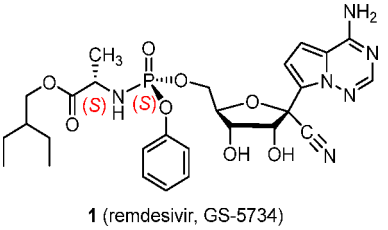

1 (remdesivir, GS-5734)

Figure 1. Structure of remdesivir **1**.

Received: December 4, 2020
Published: February 26, 2021

https://dx.doi.org/10.1021/acs.joc.0c02888
J. Org. Chem. 2021, 86, 4977−4985

against Ebola virus.[18] Remdesivir **1** is a prodrug of nucleotide (ProTide) with high cell permeability and is a promising therapeutic agent against SARS, MERS, and SARS-CoV-2.[19−21] It is metabolized inside the host cell to the corresponding nucleotide triphosphate (NTP) and targets the RdRp enzyme to inhibit viral replication within the cell.[15] The (S)-P-1 isomer plays a crucial role in RdRp inhibition in comparison with its (R)-P-isomer with respect to potency, toxicity, rate of metabolism, and phosphorylation in vivo.[22]

The synthesis of remdesivir **1** has been developed by Gilead Sciences.[16,17] Scheme 1 describes the key step of (*S*)-P-phosphoamidation, which requires high diastereomeric purity at the phosphorus center. Coupling of 2-ethylbutyl-L-alanine **2** with $PO(OPh)Cl_2$ **3** in Et_3N and CH_2Cl_2 yielded the phosphoramidoyl chloridate **4**, which was directly treated with *p*-nitrophenol in one pot to give the 1/1 mixture of diastereomers **5** (80%) after column chromatography purification. The diastereomeric mixture **5** was initially separated by HPLC using a chiral column to deliver a small amount of optically pure **6**, which was used as a seed for further resolution of **5** through selective crystallization in diisopropyl ether several times to furnish **6** in 39% yield.

Scheme 1. Stereoselective Phosphoamidation in Gilead's Synthesis of Remdesivir

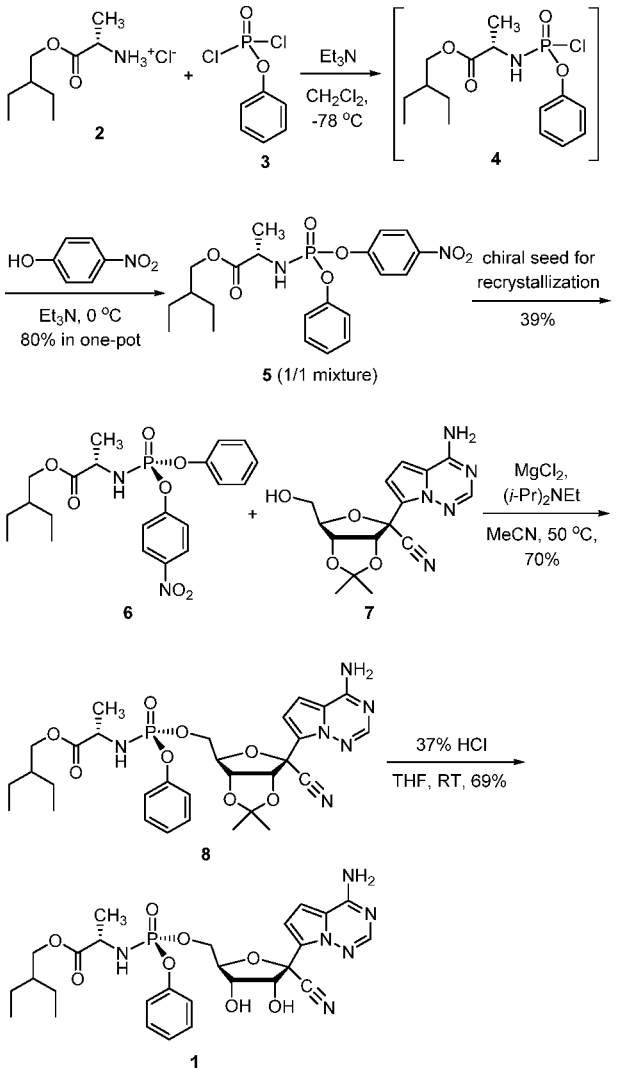

Coupling of **6** with the D-ribose-derived 5-alcohol **7** in the presence of $MgCl_2$ and diisopropylethylamine afforded the (*S*)-P-phosphoamidate **8** (70%), which underwent acidic cleavage of the isopropylidene group to provide remdesivir **1** (69%).

However, there are some drawbacks in this synthetic route: (1) an additional nucleophile, such as *p*-nitrophenol, must be employed for the stabilization of phosphoramidoyl chloridate **4**, (2) the corresponding diastereomeric mixture **5** has to be purified by silica gel column chromatography before crystallization, (3) multiple crystallization steps of the 1/1 diastereomeric mixture **5** are necessary to isolate the desired pure diastereomer **6**, resulting in a significant wastage of materials (61%), (4) the products require purification by column chromatography in the last two steps, respectively, and (5) the overall yield for the last two steps is 48.3%, which may not be considered economic-friendly. Therefore, developing an efficient methodology to improve the (*S*)-P-phosphoamidation step is important for the practical synthesis of remdesivir.

We report here a one-pot catalytic asymmetric phosphoramidation method to improve the overall synthesis. This work is inspired by the mechanism of histidine-dependent glucose 6-phosphatase catalyzed hydrolysis of glucose 6-phosphate through intermediates **9**, **10**, and **11** (Scheme 2) and the imidazole residues of His^{119} and His^{176} as proton donor and acceptor, respectively.[23] The aforementioned mechanism prompted us that chiral imidazole-derived compounds may serve as potential catalysts for stereoselective phosphoramidation. Toward our survey in this direction, we have come across few reports that the chiral bicycloimidazole-based catalysts had gained a proven ability to be employed as tailor-made motifs and can impart promising levels of stereoselectivity at phosphorus.[24,25] The desired (*R*)-stereochemistry at phosphorus had been achieved by DiRocco and co-workers, employing these kinds of chiral catalysts, which also possess (*R*)-stereochemistry.[26] On the basis of this clue, we envisioned that for the synthesis of remdesivir **1**, the need of a potential strategy to acquire the desired (*S*)-stereochemistry at phosphorus is in high demand, and we hypothesized that this could be achieved by employing the chiral (*S*)-bicycloimidazole-based catalysts as tools.

Scheme 2. Mechanism of Glucose 6-Phosphatase

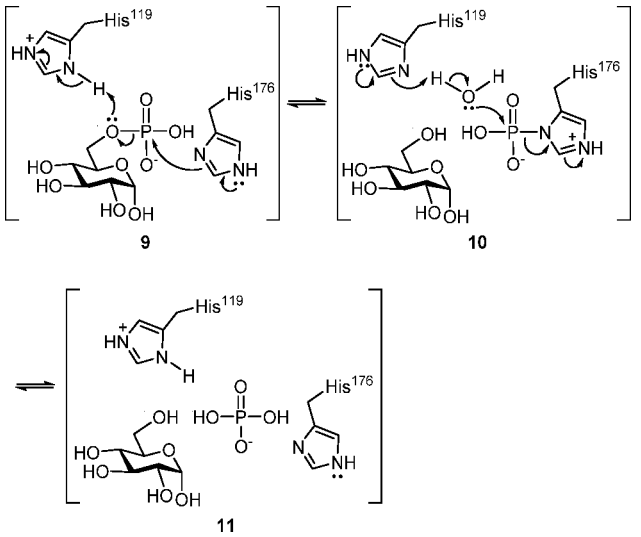

https://dx.doi.org/10.1021/acs.joc.0c02888
J. Org. Chem. 2021, 86, 4977−4985

The strategies for the assembly of P-chirogenic phosphoramidates are depicted in Scheme 3. Path A describes Gilead's approach to convert the racemic phosphoramidoyl chloridate **12** into a 1:1 mixture of **13** and **14** for further resolution to obtain enantiomer **14** for the S_N2-like coupling with alkoxide (R^1O^-) to afford the expected phosphoramidate **15**.[16,17] In Path B, employment of the chiral imidazole-derived nucleophile (Nu*) as catalyst to couple the racemic phosphoramidoyl chloridate **12** with R^1OH would give **15** through an intermolecular equilibrium of the intermediates **16** and **17**. The formation of the preferred intermediate **17** was stereoselectively controlled by the chiral environment of the catalyst. Alternatively, a chiral bis-imidazole catalyst, proposed in Path C, would offer an intramolecular equilibrium of intermediates **18** and **19**. Very importantly, both Path B and Path C utilize racemic mixture **12** as the coupling reagent without further resolution. Most recently, an imidazole-acrolein-based adamantyl-(*S*)-carbamate was developed by Zhang's group.[27] Unlike earlier described protocols, we report herein the discovery of chiral imidazole-cinnamaldehyde-derived structures as improved catalysts for the efficient synthesis of remdesivir via asymmetric (*S*)-phosphoramidation and acidic hydrolysis in a one-pot manner.

Scheme 3. Strategies for the Synthesis of P-Chirogenic Phosphoramidate

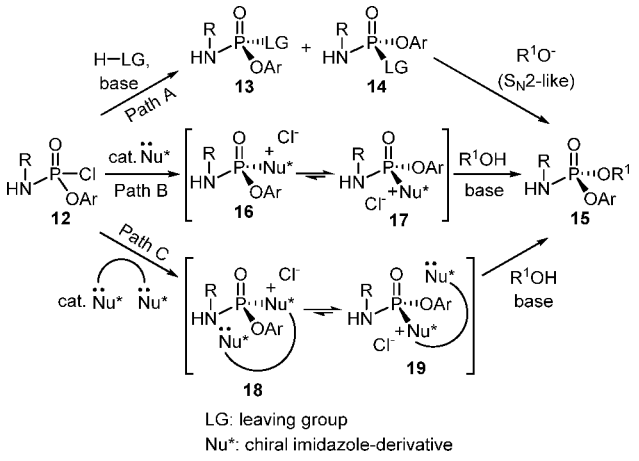

RESULTS AND DISCUSSION

A series of chiral bicyclic imidazoles and bis bicyclic imidazoles proposed for use are summarized in Figure 2. Reaction of imidazole with acrolein or cinnamaldehyde furnished a racemic mixture of bicyclic alcohols, which were separated by MPLC chiral column to yield the optically pure compounds **20**–**25**, respectively. The detailed synthetic procedures and purification methods are described in the Supporting Information. The absolute configuration of **22** was determined by X-ray single crystal analysis of its (+)-*O*-acetyl-L-mandelate derivative **26** (see the Supporting Information). Coupling of the alcohols **20**–**25** with commercially available *t*-butyl isocyanate gave the carbamates **27**–**32**, respectively. Consecutive Curtius rearrangement of the dicarboxylic acid **33** followed by coupling with the alcohols **20**–**25** delivered the bis-carbamate derivatives **34**–**39**, respectively. Benzylation and silylation of alcohol **22** provided the ether derivatives **40** and **41**, respectively.

Having the chiral catalysts in hand, the catalytic stereoselective assembly of the 1:1 phosphoramidoyl chloridates **4** with the D-ribose-derived 5-alcohol **7** in the presence of 2.0 equiv of 2,6-lutidine was systematically investigated, and the results were summarized in Table 1. In entry 1, when 20 mol % of the (*S*)-carbamate **27** was used in the reaction at −20 °C for 24 h, a mixture of the diastereomers **8** and **42** was obtained in 94% yield with 14.6/1 d.r. ratio (determined by HPLC). In contrast, the (*R*)-carbamate **28** gave 64% yield with 1.9/1 d.r. ratio (entry 2). Obviously, the (*S*)-configuration of **27** favored the formation of (*S*)-P-diastereomer with high selectivity and yield. We then tried the (*S*)-carbamate **29** having an extra phenyl group with (*R*)-configuration under similar conditions (entry 3), and the d.r. ratio (24.6/1) and yield (97%) were

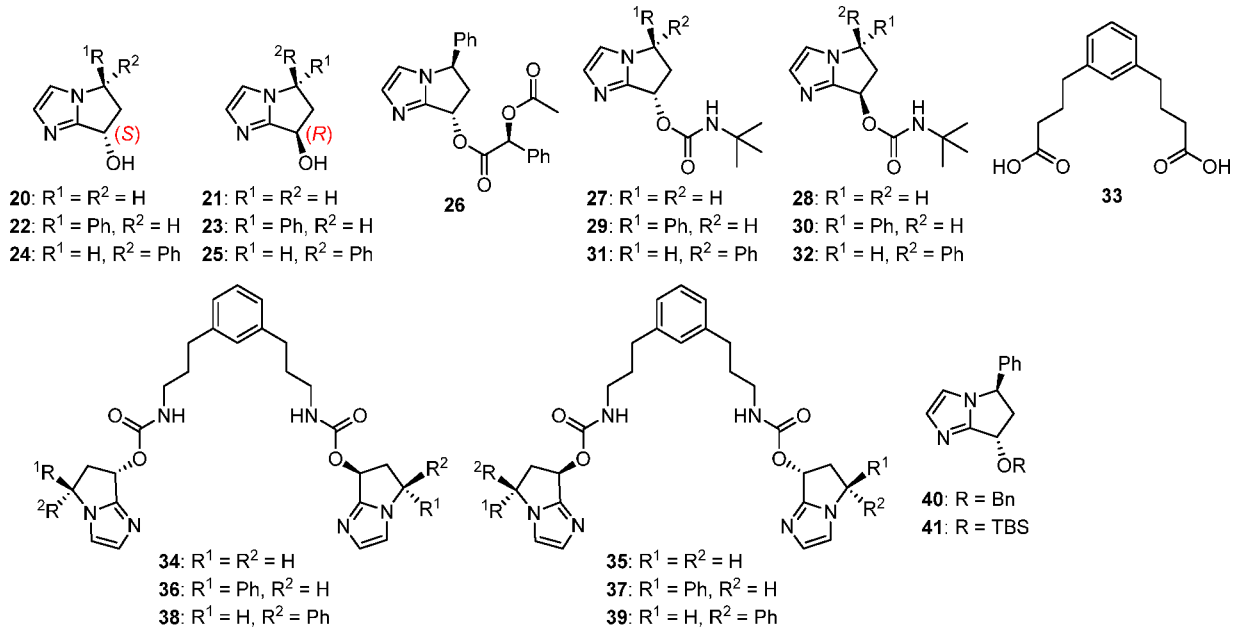

Figure 2. Structures of the imidazole-derived chiral alcohols and various chiral catalysts.

https://dx.doi.org/10.1021/acs.joc.0c02888
J. Org. Chem. 2021, 86, 4977−4985

Table 1. Results of Various Chiral Bicyclic Imidazoles as Catalysts for Stereoselective Coupling of Compounds 4 and 7

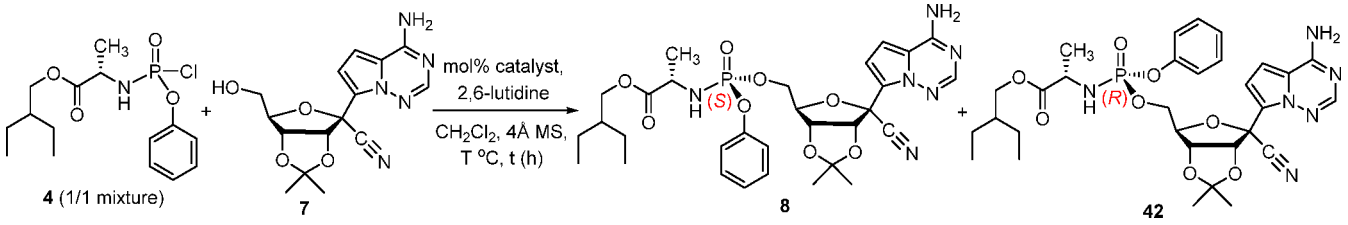

entry	catalyst	mol %	T (°C)	t (h)	yield (%)[a]	d.r. ratio (**8**/**42**)[a]
1	**27**	20	−20	24	94	14.6/1
2	**28**	20	−20	24	64	1.9/1
3	**29**	20	−20	24	97	24.6/1
4	**30**	20	−20	24	65	1.2/1
5	**31**	20	−20	24	79	14.6/1
6	**32**	20	−20	24	42	0.9/1
7	**34**	20	−20	24	94	11/1
8	**35**	20	−20	24	88	0.1/1
9	**36**	20	−20	24	96	24.6/1
10	**37**	20	−20	24	96	0.4/1
11	**38**	20	−20	24	93	5.5/1
12	**39**	20	−20	24	92	0.2/1
13	**40**	20	−20	24	68	4.9/1
14	**41**	20	−20	24	61	4.1/1
15	**26**	20	−20	24	67	3/1
16	**29**	20	−10	24	90	17.1/1
17	**29**	20	−40	48	92	30.3/1
18	**29**	20	−78	48	0	0/0
19	**29**	2	−20	55	79	4.4/1
20	**29**	10	−20	24	64	6.2/1
21	**29**	15	−20	30	93	22.8/1
22	**29**	50	−20	12	93	33.5/1
23	**29**	50	−40	24	95	36/1
24	**29**	100	−40	24	95	42.4/1

[a]The percentage (%) and ratio were determined by HPLC analysis.

slightly increased in comparison with **27**. On the other hand, in entry 5, when the (*S*)-carbamate **31** with an extra (*S*)-phenyl group was tested, a decrease in yield (79%) and 8.9/1 d.r. ratio was observed. The configuration of this extra phenyl group is important for the asymmetric phosphoramidation. We next examined the (*R*)-carbamates **30** [entry 4, (*S*)-Ph] and **32** [entry 6, (*R*)-Ph], and similar results were found as compared to **28** (entry 2). Regarding the use of bis-bicyclic imidazoles as catalysts, the d.r. ratios of **8**/**42** obtained were 11/1 (entry 7, 94% yield), 24.6/1 d.r. (entry 9, 96% yield), and 5.5/1 d.r. (entry 11, 93% yield) using the dimeric (*S*)-carbamates **34**, **36**, and **38**, respectively. Interestingly, the dimeric (*R*)-carbamates **35** (entry 8), **37** (entry 10), and **39** (entry 12) furnished the undesired diastereomer **42** as a major product in much better yields and ratios in comparison with the monomeric (*R*)-carbamates **28**, **30**, and **32**, respectively. In addition to the carbamate moiety, the (*S*)-benzyl ether (**40**, entry 13), (*S*)-silyl ether (**41**, entry 14), and (*S*)-ester (**26**, entry 15) were further investigated for the reaction to provide **8**/**42** with d.r. ratios in 4.9/1 (68%), 4.1/1 (61%), and 3/1 (67%), respectively.

Since compound **29** provides the best results in our catalyst screening in terms of yield and selectivity, we continued to study its catalytic properties as well as temperature effect. When the reaction was carried out at −10 °C (entry 16), the yield (90%) and selectivity (17.1/1) slightly decreased, whereas at a lower temperature (−40 °C), little improvement in selectivity (30.3/1) was observed (entry 17). However, the reaction required 48 h for completion due to the decrease of catalytic activity. Moreover, no reaction was observed at −78 °C (entry 18). In entries 19−24, various catalyst concentrations were studied. When the catalyst **29** was reduced to 15 mol % (entry 21), 10 mol % (entry 20) or 2 mol % (entry 19), both selectivity and yield decreased correspondingly. When 50 mol % of **29** was used at −20 °C (entry 22), the selectivity slightly increased from 24.6/1 to 33.5/1 and the reaction was completed in 12 h. By lowering the temperature to −40 °C (entry 23), a selectivity ratio of 36/1 was obtained. A similar result was observed by employing 100 mol % of **29** (entry 24), which gave a selectivity ratio of 42.4/1.

In order to avoid the purification of the mixed diastereomers **8** and **42**, a one-pot synthesis of remdesivir was investigated (Scheme 4). In a 1-g scale synthesis, compounds **4** and **7** were coupled in the presence of catalyst **29** followed by acidic hydrolysis in *p*-TSA and methanol at room temperature to remove the isopropylidene group in the same reaction flask to furnish a mixture of **1** and its (*R*)-diastereomer in 96.1/3.9 d.r., which was further purified via recrystallization to give remdesivir **1** (73%) in 99.4/0.6 d.r. The catalyst **29** was recovered in 82% yield for reuse with similar efficacy. A 10-g scale synthesis was then performed with the same protocols, and consistent results were obtained to give **1** and **29** in 70% (99.3/0.7 d.r.) and 83% yields, respectively.

https://dx.doi.org/10.1021/acs.joc.0c02888
J. Org. Chem. 2021, 86, 4977−4985

Scheme 4. One-Pot Synthesis of Remdesivir

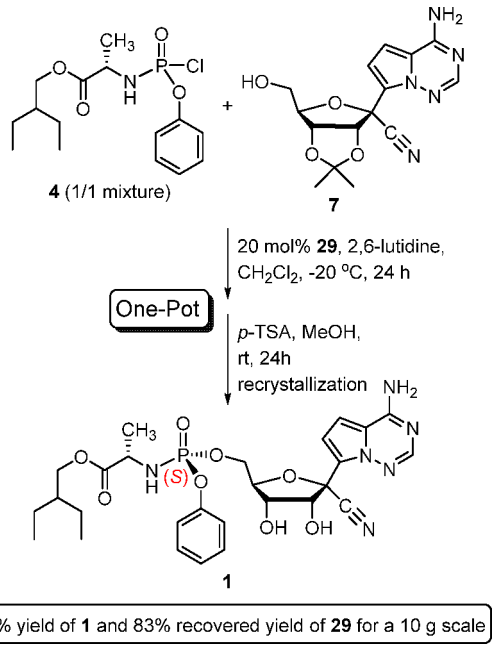

CONCLUSION

In conclusion, the chiral carbamate **29**, derived from imidazole and cinnamaldehyde in two steps, was successfully developed as an efficient catalyst for the stereoselective (*S*)-P-phosphoramidation in excellent yield and selectivity. The 1/1 mixture of phosphoramidoyl chloridates **4** could be directly used as the coupling reagent, avoiding a waste of the other diastereomer. In addition, a high yielding combination of (*S*)-P-phosphoramidation and isopropylidene-deprotection successfully provided remdesivir in a one-pot manner. The organocatalyst **29** could be recovered in good yield, and similar results were obtained using the recovered catalyst. This one-pot process is relatively easy to scale up, and is expected to have a great potential for industrial development.

EXPERIMENTAL SECTION

General Information. All reactions were performed under an atmosphere of nitrogen/argon in flame-dried glassware. Solvents were distilled in the standard way, and commercial reagents were used without any purification unless otherwise stated. Anhydrous solvents like CH_2Cl_2, Et_2O, DMF, and Et_3N were dried in a standard way. TLC was performed on glass plates precoated with Silica Gel 60 F_{254} (0.25 mm, E. Merck). TLC plates were visualized by exposure to ultraviolet light (UV-254 nm) and/or submersion in aqueous potassium permanganate solution ($KMnO_4$) followed by heating on a hot plate (120 °C). Flash column chromatography was carried out on Silica Gel 60 (230−400 mesh, E. Merck) or MPLC (INTERCHEM250). Crystal structure was recorded on single-crystal X-ray diffractometer (Brucker CCD). ^{1}H NMR spectra were recorded on 600 MHz instrument at ambient temperature. Data were recorded as follows: chemical shift in ppm from the solvent resonance employed as the internal standard ($CDCl_3$ at 7.26 ppm, and CD_3OD at 3.35 and 4.78 ppm), multiplicity (s = singlet, d = doublet; t = triplet; q = quartet; st = septet; m = multiplet; br = broad), coupling constant (Hz), integration. ^{13}C NMR spectra were measured on 150 MHz spectrometer. Chemical shifts were recorded in ppm from the solvent resonance employed as the internal standard ($CDCl_3$ at 77.23 ppm, and CD_3OD at 49.3 ppm). Mass spectra were obtained with ESI Finnigan LCQ mass spectrometer (Thermo Finnigan), performed at Genomics Research Center. Chiral HPLC analysis were performed using an HPLC system (HP-2100, Agilent), consisting of a quaternary gradient pump (Agilent 1100), conductivity detector (PROD, AERS500, 4 mm, Thermal), reagent-free controller (PROD. RFC10) and autosampler (Agilent 1260 infinity) system with and acetonitrile−water mobile phase and UV detection.

Synthesis of Compounds 20 and 21.[28] To a mixture of imidazole (50.0 g, 0.74 mol) and acetic acid (2.9 mL, 0.051 mol) in dioxane (500 mL) was added acrolein (73.0 mL, 1.09 mol) at room temperature. The resulting solution was then refluxed on oil bath for 36 h. After cooling to room temperature, the mixture was concentrated under reduced pressure, and the crude residue was subjected to flash column chromatography on silica gel by using ethyl acetate/CH_2Cl_2/hexane (5/1/5 → 7/2/1) to give an enantiomeric mixture, which was purified by MPLC chiral OD-H column to yield **20** (37.0 g, 40.5%) and **21** (37.0 g, 40.5%).^{1}H NMR (600 MHz, $CDCl_3$) δ 7.04 (s, 1H), 6.82 (d, J = 6.0 Hz, 1H), 5.18−5.16 (m, 1H), 4.18−4.14 (m, 1H), 3.90−3.86 (m, 1H), 2.93−2.88 (m, 1H), 2.57−2.52 (m, 1H). ^{13}C{^{1}H} NMR (151 MHz, $CDCl_3$) δ 156.5, 132.8, 114.7, 64.2, 43.5, 36.5.

Synthesis of Compounds 22−25. To a solution of cinnamaldehyde (25.0 mL, 0.19 mol) and imidazole (40.5 g, 0.57 mol) in dioxane (250 mL) was added acetic acid (6.0 mL, 0.105 mol) at room temperature. The reaction mixture was vigorously refluxed on oil bath for 72 h. After cooling to room temperature, the solvent was evaporated under reduced pressure. The crude residue was dissolved in CH_2Cl_2, and washed with saturated $NaHCO_3$ solution. The organic layer was dried over $MgSO_4$, filtered, and concentrated in vacuo. The crude residue was treated with 80% ethyl acetate in hexane and sonicated for 30 min. The resultant solids were filtered and washed with cold ethyl acetate. The solids were purified through the silica gel column chromatography by using ethyl acetate/dichloromethane/hexane (5/1/4) as the eluent to afford the *trans*-isomers (18.2 g, 46.2%) and *cis*-isomers (9.8 g, 23.8%), respectively. Both isomers were identified by the NOESY spectra.

trans-isomers: ^{1}H NMR (600 MHz, $CDCl_3$) δ 7.38−7.36 (m, 2H), 7.33−7.30 (m, 3H), 7.11 (s, 1H), 6.66 (s, 1H), 5.37−5.35 (m, 1H), 5.17−5.15 (m, 1H), 3.47−3.40 (m, 1H), 2.58−2.54 (m, 1H). ^{13}C{^{1}H} NMR (151 MHz, $CDCl_3$) δ 156.6, 140.4, 133.5, 129.2, 128.6, 126.9, 114.0, 64.5, 59.8, 46.5.

cis-isomers: ^{1}H NMR (600 MHz, $CDCl_3$) δ 7.38−7.32 (m, 3H), 7.15 (d, J = 6.0 Hz, 2H), 7.09 (s, 1H), 6.66 (s,1H), 5.51(t, J = 6.8 Hz, 1H), 5.42 (d, J = 6.0 Hz, 1H), 3.05−3.01 (m, 1H), 2.82−2.77 (m, 1H). ^{13}C{^{1}H} NMR (151 MHz, $CDCl_3$) δ 156.6, 140.2, 133.1, 129.2, 128.5, 126.4, 114.1, 64.5, 60.0, 48.1.

Separation and Identification of *trans*-Enantiomers 22 and 23. The enantiomers **22** and **23** were separated by MPLC Chiral OD-H column using IPA/hexane (3/7) as an eluent. To identify the stereochemistry of the separated enantiomers **22** and **23**, their enantiomeric mixture was subjected to resolution by using (+)-*O*-acetyl-L-mandelic acid.

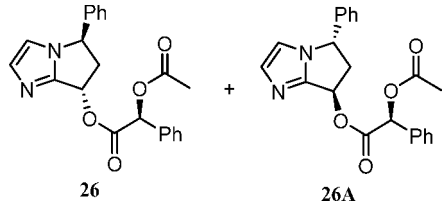

26 **26A**

To a solution of the enantiomers **22** and **23** (1.0 g, 4.99 mmol) and (+)-*O*-acetyl-L-mandelic acid in CH_2Cl_2 (10 mL) was sequentially added EDC·HCl (1.43 g, 7.40 mmol) and DMAP (0.61 g, 4.99 mmol) at 0 °C under N_2 atmosphere. After removing the ice bath, the mixture was continuously stirred at room temperature for 3 h. The reaction mixture was concentrated, and the crude residue was dissolved in ethyl acetate (20 mL). The mixture was washed with saturated $NaHCO_3$ solution, and the organic layer was dried over $MgSO_4$, filtered, and concentrated in vacuo. The crude mixture was subjected to silica gel column chromatography using ethyl acetate/hexane (1/3) as eluent to afford **26** (820 mg, 44%) as a semi solid and **26A** (790 mg, 42%) as a gummy solid.

https://dx.doi.org/10.1021/acs.joc.0c02888
J. Org. Chem. 2021, 86, 4977−4985

Compound **26**: ^{1}H NMR (600 MHz, $CDCl_3$) δ 7.49 (d, J = 4.3 Hz, 2H), 7.44−7.36 (m, 6H), 7.22 (s, 1H), 7.15 (d, J = 6.7 Hz, 2H), 6.78 (d, J = 0.6 Hz, 1H), 6.10 (d, J = 6.5 Hz, 1H), 5.87 (s, 1H), 5.47 (t, J = 6.9 Hz, 1H), 3.11 (dd, J = 14.7, 6.8 Hz, 1H), 2.91 (dt, J = 13.9, 6.8 Hz, 1H), 2.23 (s, 3H). $^{13}C\{^1H\}$ NMR (151 MHz, $CDCl_3$) δ 171.0, 168.8, 150.3, 139.3, 135.4, 133.0, 129.7, 129.4, 129.1, 128.9, 127.9, 126.5, 115.4, 75.0, 68.9, 59.6, 46.1, 20.9. HRMS m/z (ESI, M + Na^+) calcd for $C_{22}H_{20}N_2O_4Na^+$ 399.1321, found 399.1330.

Compound **26A**: ^{1}H NMR (600 MHz, $CDCl_3$) δ 7.44 (dd, J = 6.5, 2.9 Hz, 2H), 7.39−7.36 (m, 3H), 7.35−7.29 (m, 3H), 7.20 (s, 1H), 7.05−6.99 (m, 2H), 6.71 (d, J = 0.6 Hz, 1H), 6.10 (dd, J = 6.5, 1.8 Hz, 1H), 5.15 (t, J = 6.9 Hz, 1H), 2.77 (dt, J = 13.6, 6.7 Hz, 1H), 2.70 (dd, J = 14.7, 6.9, 1.8 Hz, 1H), 2.15 (s, 3H). $^{13}C\{^1H\}$ NMR (151 MHz, $CDCl_3$) δ 170.3, 168.5, 150.4, 139.1, 135.5, 133.8, 129.6, 129.4, 129.1, 129.0, 128.0, 126.4, 115.4, 74.6, 68.7, 59.5, 45.9, 20.9. HRMS m/z (ESI, M + Na^+) calcd for $C_{12}H_{12}N_2ONa^+$ 399.1321, found 399.1329.

The compound **26** was subjected to crystallization by using vapor diffusion method ($CHCl_3$/Hexane) and crystal growth is in monoclinic form (Table S1). The crystal structure of compound **26** has revealed that its corresponding precursor after treating with sodium hydroxide in methanol is compound **22**, which is the peak-2 in the MPLC chromatogram. The other peak should be compound **23**.

Separation and Identification of *cis*-Enantiomers 24 and 25. The enantiomers **24** and **25** were separated by employing the MPLC Chiral OD-H column using IPA/hexane (3/7) as an eluent. The separated *cis*-enantiomers **24** and **25** were subjected to Mitsunobu reaction followed by saponification to furnish the epimers **23** and **22**, respectively.

General Procedure (A) for the Synthesis of Compounds 27 and 28. To a solution of an alcohol (50 mg, 0.40 mmol) in THF (1.0 mL) was added sodium hydride (60% in mineral oil, 19 mg, 0.48 mmol) in portions. After 30 min, *tert*-butylisocyanate (40 mg, 0.40 mmol) was added dropwise. After 16 h, the reaction was quenched by water (2.0 mL), and the mixture was then partitioned between water (2.0 mL) and *i*-PrAc (4.0 mL). The organic layer was washed with brine (4.0 mL), dried over $MgSO_4$, filtered, and concentrated to yield a pale orange semisolid. The residue was dissolved in MTBE (2.0 mL) with gentle heating on water bath, and heptane (2.0 mL) was added to the mixture over 10 min. After 2 h, the mixture was filtered, and the filtrate was washed with 1/1 MTBE/heptane (2 mL) and dried under nitrogen stream to yield the desired compound.

Compound 27. Compound **27** was prepared according to the general procedure (A) as a white solid (77 mg, 86%). ^{1}H NMR (600 MHz, $CDCl_3$) δ 7.17 (s, 1H), 6.93 (s, 1H), 5.87 (d, J = 4.8 Hz, 1H), 4.75 (s, 1H), 4.04−4.10 (m, 1H), 3.98−3.94 (m, 1H), 3.08−3.02 (m, 1H), 2.61−2.57 (m, 1H), 1.30 (s, 9H). $^{13}C\{^1H\}$ NMR (151 MHz, $CDCl_3$) δ 154.1, 151.8, 135.0, 115.6, 67.3, 50.7, 43.1, 35.6, 29.0. HRMS m/z (ESI, M + H^+) calcd for $C_{11}H_{18}N_3O_2^+$ 224.1394, found 224.1398.

Compound 28. Compound **28** was prepared according to the general procedure (A) as a white solid (79 mg, 88%). ^{1}H NMR (600 MHz, $CDCl_3$) δ 7.18 (s, 1H), 6.93 (s, 1H), 5.87 (d, J = 5.4 Hz, 1H), 4.75 (s, 1H), 4.14−4.10 (m, 1H), 3.98−3.94 (m, 1H), 3.07−3.02 (m, 1H), 2.61−2.57 (m, 1H), 1.30 (s, 9H). $^{13}C\{^1H\}$ NMR (151 MHz, $CDCl_3$) δ 154.1, 151.8, 135.0, 115.6, 67.3, 50.8, 43.1, 35.6, 29.8, 29.0. HRMS m/z (ESI, M + H^+) calcd for $C_{11}H_{18}N_3O_2^+$ 224.1394, found 224.1398.

General Procedure (B) for the Synthesis of Compounds 29−32. To a solution of an alcohol (50 mg, 0.25 mmol) and *tert*-butylisocyanate (25 mg, 0.25 mmol) in THF (3 mL) was added sodium hydride (60% in mineral oil, 7.2 mg, 0.30 mmol) at room temperature under N_2 atmosphere. After 30 min, the reaction was quenched by water (2 mL), and the mixture was concentrated in vacuo to give a pale orange semisolid. The crude residue was purified by silica gel chromatography using EtOAc/hexane (3/1) as the eluent to provide the desired product.

Compound 29. Compound **29** was prepared according to the general procedure (B) and purified by column chromatography by using EtOAc/hexane (3/1) to afford **29** as a white solid (66 mg, 89%). ^{1}H NMR (600 MHz, $CDCl_3$) δ 7.40−7.36 (m, 3H), 7.24 (s, 1H), 7.14 (d, J = 6.1 Hz, 2H), 6.78 (s, 1H), 6.03 (d, J = 5.7 Hz, 1H), 5.44 (t, J = 6.0 Hz, 1H), 4.81 (s, 1H), 3.08−3.04 (m, 1H), 2.92−2.87 (m, 1H), 1.34 (s, 9H). $^{13}C\{^1H\}$ NMR (151 MHz, $CDCl_3$) δ 153.9, 151.8, 139.6, 135.1, 129.4, 128.8, 126.4, 115.1, 67.2, 59.6, 50.7, 46.6, 29.0. HRMS m/z (ESI, M + H^+) calcd for $C_{17}H_{22}N_3O_2^+$ 300.1707, found 300.1712.

Compound 30. Compound **30** was prepared according to the general procedure (B) and purified by column chromatography by using EtOAc/hexane (3/1) to afford **30** as a white solid (62 mg, 87%). ^{1}H NMR (600 MHz, $CDCl_3$) δ 7.38−7.32 (m, 3H), 7.21 (s, 1H), 7.18 (d, J = 6.0 Hz, 2H), 6.77 (s, 1H), 5.98−5.97 (m, 1H), 5.23−5.20 (m, 1H), 4.79 (s, 1H), 3.60−3.55 (m, 1H), 2.49−2.47 (m, 1H), 1.29 (s, 9H). $^{13}C\{^1H\}$ NMR (151 MHz, $CDCl_3$) δ 154.0, 151.8, 140.5, 135.4, 129.3, 128.7, 126.4, 115.0, 67.2, 59.3, 50.8, 45.7, 29.8, 29.0. HRMS m/z (ESI, M + H^+) calcd for $C_{17}H_{22}N_3O_2^+$ 300.1707, found 300.1706.

Compound 31. Compound **31** was prepared according to the general procedure (B) and purified by column chromatography by using EtOAc/hexane (3/1) to afford **31** as a white solid (62 mg, 87%). ^{1}H NMR (600 MHz, $CDCl_3$) δ 7.40−7.36 (m, 3H), 7.24 (s, 1H), 7.14 (d, J = 6.0 Hz, 2H), 6.78 (s, 1H), 6.03 (d, J = 5.2 Hz, 1H), 5.42 (t, J = 6.0 Hz, 1H), 4.80 (s, 1H), 3.08−3.04 (m, 1H), 2.92−2.87 (m, 1H), 1.34 (s, 9H). $^{13}C\{^1H\}$ NMR (151 MHz, $CDCl_3$) δ 153.96, 151.85, 139.70, 135.254, 129.36, 128.79, 126.37, 115.11, 67.23, 59.64, 50.78, 46.66, 29.02. HRMS m/z (ESI, M + H^+) calcd for $C_{17}H_{22}N_3O_2^+$ 300.1707, found 300.1715.

Compound 32. Compound **32** was prepared according to the general procedure (B) and purified by column chromatography by using EtOAc/hexane (3/1) to afford **32** as a white solid (61 mg, 85%). ^{1}H NMR (600 MHz, $CDCl_3$) δ 7.38−7.33 (m, 3H), 7.26 (s, 1H), 7.21−7.17 (m, 2H), 6.77 (s, 1H), 5.97 (dd, J = 12.2, 6.8 Hz, 1H), 5.21 (dd, J = 12.0, 6.0 Hz, 1H), 4.78 (s, 1H), 3.59−3.56 (m, 1H), 2.48 (dd, J = 12.0 Hz, 6.0 Hz, 1H), 1.30 (s, 9H). $^{13}C\{^1H\}$ NMR (151 MHz, $CDCl_3$) δ 154.0, 151.8, 140.5, 135.4, 129.3, 128.7, 126.4, 115.0, 67.3, 59.3, 50.8, 45.7, 29.8, 29.0. HRMS m/z (ESI, M + H^+) calcd for $C_{17}H_{22}N_3O_2^+$ 300.1707, found 300.1702.

General Procedure (C) for the Synthesis of Compounds 34−39. 4,4′-(1,3-Phenylene)dibutanoic acid (200 mg, 0.80 mmol) and triethylamine (0.25 mL, 1.80 mmol) were dissolved in THF (4.0 mL) under N_2 atmosphere. After cooling to 0 °C, ethyl chloroformate (0.17 mL, 1.80 mmol) was added, and the mixture was stirred for 30 min. To this mixture was added a solution of sodium azide (0.26 g, 4.0 mmol) in water (3.4 mL). After 30 min, toluene (10 mL) and water (10 mL) were added, and the organic layer was separated. The aqueous layer was extracted with toluene (3 × 10 mL), and the combined organic layers were dried over $MgSO_4$, filtered, and concentrated to ∼50% of the original volume. The crude solution of the acyl azide was then heated to 90 °C on oil bath for 30 min, then concentrated to yield the diisocyanate (195 mg, 90%) as a yellow oil. THF (4.0 mL) was added to dissolve the residue, and the corresponding starting material among (**20**−**25**) (1.6 mmol) and sodium hydride (60% suspension in mineral oil, 14 mg, 0.36 mmol) were sequentially added to the mixture. An additional portion of sodium hydride was added to complete the reaction. After 30 min, a few drops of water were added to quench the reaction, and the solvent was removed in vacuo. The crude residue was purified by silica gel chromatography using EtOAc/hexane (3/1) as the eluent to provide the desired product.

Compound 34. Compound **34** was prepared according to the general procedure (C) and purified by column chromatography by using EtOAc/hexane (3/1) to afford **34** as a white solid (299 mg, 76%). ^{1}H NMR (600 MHz, $CDCl_3$) δ 7.17−7.15 (m, 3H), 7.0−6.93 (m, 5H), 5.90−5.87 (m, 2H), 5.17−4.95 (m, 2H), 4.14−4.09 (m, 2H), 3.98−3.95 (m, 2H), 3.24−3.12 (m, 4H), 3.08−3.00 (m, 2H), 2.61−2.57 (m, 6H), 1.83−1.77 (m, 4H). $^{13}C\{^1H\}$ NMR (151 MHz, $CDCl_3$) δ 155.9, 151.7, 142.1, 141.6, 135.0, 134.8, 128.9, 128.8, 126.3, 126.3, 115.6, 67.9, 43.1, 40.7, 39.8, 35.5, 35.4, 33.1, 32.9, 31.9, 31.6,

https://dx.doi.org/10.1021/acs.joc.0c02888
J. Org. Chem. 2021, 86, 4977−4985

31.4. HRMS m/z (ESI, M + H^+) calcd for $C_{26}H_{33}N_6O_4^+$ 493.2558, found 493.2556.

Compound 35. Compound **35** was prepared according to the general procedure (C) and purified by column chromatography by using EtOAc/hexane (3/1) to afford **35** as a white solid (295 mg, 75%). ^{1}H NMR (600 MHz, $CDCl_3$) δ 7.20−7.15 (m, 3H), 7.0−6.93 (m, 5H), 5.90−5.89 (m, 2H), 4.97 (bs, 2H), 4.14−4.10 (m, 2H), 3.98−3.94 (m, 2H), 3.25−3.13 (m, 2H), 3.08−3.02 (m, 2H), 2.62−2.57 (m, 6H), 1.84−1.77 (m, 4H). ^{13}C{^{1}H} NMR (151 MHz, $CDCl_3$) δ 155.9, 151.7, 141.6, 134.9, 128.8, 126.3, 115.6, 77.4, 77.2,77.0, 67.9, 43.1, 40.7, 35.5, 33.1, 31.6. HRMS m/z (ESI, M + H^+) calcd for $C_{26}H_{33}N_6O_4^+$ 493.2558, found 493.2560.

Compound 36. Compound **36** was prepared according to the general procedure (C) and purified by column chromatography by using EtOAc/hexane (3/1) to afford **36** as a white solid (278 mg, 54%). ^{1}H NMR (600 MHz, $CDCl_3$) δ 7.38−7.34 (m, 6H), 7.26 (bs, 2H), 7.11 (bs, 4H), 7.01(bs, Hz, 3H), 6.74 (s, 2H), 6.02 (s, 2H), 5.40 (bs, 1H), 5.04 (bs, 2H), 3.20−3.18 (m, 4H), 3.05−3.02 (m, 2H), 2.89−2.85 (m, 2H), 2.62 (t, J = 6.2 Hz, 4H), 2.47 (t, J = 5.7 Hz, 4H). ^{13}C{^{1}H} NMR (151 MHz, $CDCl_3$) δ 155.8, 151.7, 141.7, 139.7, 135.3, 129.4, 128.8, 128.79, 128.7, 126.4, 126.3, 115.1, 67.9, 59.6, 46.6, 40.8, 33.1, 31.6. HRMS m/z (ESI, M + H^+) calcd for $C_{38}H_{41}N_6O_4^+$ 645.3184, found 645.3173.

Compound 37. Compound **37** was prepared according to the general procedure (C) and purified by column chromatography by using EtOAc/hexane (3/1) to afford **37** as a white solid (288 mg, 56%). ^{1}H NMR (600 MHz, $CDCl_3$) δ 7.38−7.34 (m, 6H), 7.26 (d, J = 5.9 Hz, 2H), 7.11 (d, J = 6.0 Hz, 4H), 7.01(d, J = 6.0 Hz, 4H), 6.75 (s, 1H), 6.02 (d, J = 5.2 Hz, 2H), 5.40 (t, J = 6.1 Hz, 2H), 4.94 (bs, 2H), 3.25−3.18 (m, 4H), 3.05−3.02 (m, 2H), 2.89−2.85 (m, 2H), 2.62 (t, J = 6.2 Hz, 4H), 2.47 (t, J = 5.7 Hz, 4H). ^{13}C{^{1}H} NMR (151 MHz, $CDCl_3$) δ 155.8, 151.7, 141.7, 139.7, 135.3, 129.4, 128.8, 128.8, 128.7, 126.4, 126.3, 115.1, 67.9, 59.6, 46.6, 40.8, 33.1, 31.6. HRMS m/z (ESI, M + H^+) calcd for $C_{38}H_{41}N_6O_4^+$ 645.3184, found 645.3177.

Compound 38. Compound **38** was prepared according to the general procedure (C) and purified by column chromatography by using EtOAc/hexane (3/1) to afford **38** as a white solid (293 mg, 57%). ^{1}H NMR (600 MHz, $CDCl_3$) δ 7.34−7.33 (m, 6H), 7.25 (s, 2H), 7.20−7.15 (m, 5H), 6.96 (bs, 3H), 6.77 (s, 2H), 5.99 (s, 2H), 5.20 (s, 2H), 4.98 (s, 2H), 3.56−3.55 (m, 2H), 3.20−3.14 (m, 4H) 2.58−2.47 (m, 6H), 1.8 (bs, 4H). ^{13}C{^{1}H} NMR (151 MHz, $CDCl_3$) δ 155.8, 151.7, 141.7, 139.7, 135.2, 129.4, 128.8, 128.8, 126.4, 126.2, 115.1, 67.8, 59.6, 46.5, 40.8, 33.1, 31.6. HRMS m/z (ESI, M + H^+) calcd for $C_{38}H_{41}N_6O_4^+$ 645.3184, found 645.3190.

Compound 39. Compound **39** was prepared according to the general procedure (C) and purified by column chromatography by using EtOAc/hexane (3/1) to afford **39** as a white solid (283 mg, 55%). ^{1}H NMR (600 MHz, $CDCl_3$) δ 7.34−7.33 (m, 6H), 7.25 (s, 2H), 7.20−7.15 (m, 5H), 6.96 (bs, 3H), 6.77 (s, 2H), 5.99 (s, 2H), 5.20 (s, 2H), 4.98 (s, 2H), 3.56−3.55 (m, 2H), 3.20−3.14 (m, 4H) 2.58−2.47 (m, 6H), 1.8 (bs, 4H). ^{13}C{^{1}H} NMR (151 MHz, $CDCl_3$) δ 155.8, 151.7, 141.7, 139.7, 135.2, 129.4, 128.8, 128.8, 126.4, 126.3, 115.1, 67.9, 59.6, 46.5, 40.8, 33.1, 31.6. HRMS m/z (ESI, M + H^+) calcd for $C_{38}H_{41}N_6O_4^+$ 645.3184, found 645.3176.

Compound 40. To a solution of the alcohol **22** (100 mg, 0.51 mmol) and benzyl chloride (104 mg, 0.75 mmol) in anhydrous THF (2.0 mL) was added NaH (9.0 mg, 0.37 mmol) at 0 °C under N_2 atmosphere. After the ice-bath was removed, resulting solution was continuously stirred at room temperature for 8 h. The mixture was quenched with ice-cold water and extracted with EtOAc (3 × 5 mL), and the combined organic layers were dried over $MgSO_4$, filtered, and concentrated in vacuo. The crude residue was subjected to silica gel column chromatography by using EtOAc/hexane (1/9 → 1/1 → 3/1) to afford the benzyl ether **40** (99 mg, 68%) as a colorless oil. ^{1}H NMR (600 MHz, $CDCl_3$) δ 7.41−7.34 (m, 7H), 7.30−7.27 (m, 1H), 7.20 (s, 1H), 7.15−7.13 (s, 2H), 6.74 (s, 1H), 5.46 (dd, J = 12.0, 6.0 Hz, 1H), 4.95−4.90 (m, 2H), 4.75−4.73 (m, 1H), 3.06−3.02 (m, 1H), 2.73−2.69 (m, 1H). ^{13}C{^{1}H} NMR (151 MHz, $CDCl_3$) δ 153.6, 139.9, 138.0, 134.2, 129.3, 128.7, 128.6, 128.3, 127.9, 126.6, 114.7, 71.5, 71.0, 59.9, 47.0, 29.9. HRMS m/z (ESI, M + H^+) calcd for $C_{19}H_{19}N_2O^+$ 291.1492, found 291.1493.

Compound 41. To a solution of the alcohol **22** (100 mg, 0.51 mmol) and 2,6-lutidine (80.4 mg, 0.75 mmol) in CH_2Cl_2(1.5 mL) was added TBDMSOTf (0.11 mL, 0.5 mmol) at 0 °C under N_2 atmosphere. The mixture was warmed to room temperature and continuously stirred for 12 h. After concentration in vacuo, the residue was subjected to silica gel chromatography by using EtOAc/hexane (1/9 → 1/1 → 3/1) to afford the desired compound **41** as a colorless liquid (99 mg, 63%). ^{1}H NMR (600 MHz, $CDCl_3$) δ 7.36−7.33 (m, 3H), 7.17 (s, 1H), 7.10 (s, 2H), 6.67 (s, 1H), 5.44 (s, 1H), 5.21 (s, 1H), 2.88−2.86 (m, 1H), 2.71−2.68 (m, 1H), 0.92 (s, 9H), 0.22 (s, 3H), 0.13 (s, 3H). ^{13}C{^{1}H} NMR (151 MHz, $CDCl_3$) δ 155.2, 140.4, 134.4, 129.3, 128.6, 126.5, 114.2, 66.3, 59.4, 49.8, 26.1, 18.5, −4.3, −4.6. HRMS m/z (ESI, M + H^+) calcd for $C_{18}H_{27}N_2OSi^+$ 315.1887, found 315.1889.

Catalytic Asymmetric Phosphoramidation and One-Pot Synthesis of Remdesivir. *Compound 4.* Compound **4** was prepared by following the reported literature.[29] ^{1}H NMR (500 MHz, $CDCl_3$) δ 7.40 (td, J = 8.2, 2.6 Hz, 2H), 7.28 (dd, J = 14.0, 7.5 Hz, 3H), 4.48−4.31 (m, 1H), 4.28−4.09 (m, 3H), 1.62−1.53 (m, 4H), 1.42−1.35 (m, 4H), 0.92 (dd, J = 13.2, 7.3 Hz, 6H). ^{31}P NMR (242 MHz, $CDCl_3$) δ 8.05 and 7.74.

General Procedure for the Catalytic Asymmetric Phosphoramidation. In a flame-dried round-bottom flask, a mixture of the 5-alcohol **7** (10.0 mg, 0.03 mmol) and catalyst (mol %, according to the Table 1) was coevaporated with anhydrous toluene (1.0 mL, 2 times), and dried under high vacuum for 2 h. The mixture was dissolved in dry CH_2Cl_2 (1.0 mL) under N_2 atmosphere, and freshly activated 4 Å molecular sieves (20 mg) and 2,6-luditine (7.0 μL, 0.06 mmol) were sequentially added to the solution. The resulting mixture was stirred at room temperature for 10 min, and then cooled to −20 °C. After 10 min, a solution of the phosphoramidoyl chloridates **4** (15.7 mg, 0.05 mmol) in dry CH_2Cl_2 (0.5 mL) was added, and the reaction mixture was continuously stirred at same temperature for 24 h. The reaction was monitored by TLC analysis until the complete consumption of the starting material **7**. The whole reaction mixture was filtered through a pad of Celite, and the filtrate was concentrated in vacuo. The crude residue was dissolved in methanol and filtered off. The filtrate was subjected to HPLC analysis.

One-Pot Synthesis of Remdesivir 1 in a 1.0 g Scale. In a flame-dried round-bottom flask, a mixture of the 5-alcohol **7** (1.0 g, 3.02 mmol) and the catalyst **29** (180 mg, 0.62 mmol) were coevaporated with anhydrous toluene (20 mL, 2 times) and dried under high-vacuum for 2 h. The mixture was dissolved in anhydrous CH_2Cl_2 (50 mL) under N_2 atmosphere, and freshly activated 4 Å molecular sieves (1.5 g) and 2,6-luditine (700 μL, 6.04 mmol) were sequentially added to the solution. The reaction mixture was stirred at room temperature for 10 min, and then cooled to −20 °C. After 10 min, a solution of the phosphoramidoyl chloridates **4** (1.57 g, 4.53 mmol) in CH_2Cl_2 (5 mL) was added, and the reaction mixture was stirred at the same temperature for 24 h. Dichloromethane was then evaporated through the needle under reduced pressure. The crude material was treated with *p*-TSA (5.74 g, 30.2 mmol) in methanol (50 mL), and the resulting solution was continuously stirred at room temperature for 24 h. The reaction mixture was filtered through a pad of Celite to remove 4 Å molecular sieves, quenched by adding triethylamine, and concentrated in vacuo. The crude residue was dissolved in EtOAc (100 mL), and the mixture was washed with saturated $NaHCO_3$. The aqueous layer was extracted with EtOAc (3 × 50 mL), and the combined organic layers were dried over $MgSO_4$, filtered and concentrated in vacuo. The crude residue was subjected to silica gel column chromatography by using EtOAc/hexane (1/9 → 1/1 → 3/1 → 1/0) to afford the catalyst **29** (148 mg, 82%) and a mixture of the diastereomers, which was further purified by recrystallization from CH_3CN and CH_2Cl_2 to afford remdesivir **1** (1.39 g, 73% yield, 99.4/0.6 d.r.) as a white solid. ^{1}H NMR (600 MHz, CD_3OD) δ 7.87 (s, 1H), 7.30 (t, J = 7.8 Hz, 2H), 7.21−7.14 (m, 3H), 6.91 (d, J = 4.6 Hz, 1H), 6.88 (d, J = 4.6 Hz, 1H), 4.79 (d, J = 5.4 Hz, 1H), 4.42−4.35 (m, 2H), 4.28 (dt, J = 10.5, 5.1 Hz, 1H),

https://dx.doi.org/10.1021/acs.joc.0c02888
J. Org. Chem. 2021, 86, 4977−4985

4.17 (t, J = 5.6 Hz, 1H), 4.02 (dd, J = 10.9, 5.8 Hz, 1H), 3.90 (ddd, J = 23.7, 12.7, 6.4 Hz, 2H), 1.45 (dt, J = 12.3, 6.2 Hz, 1H), 1.34−1.28 (m, 7H), 0.85 (t, J = 7.5 Hz, 6H). $^{13}C\{^1H\}$ NMR (151 MHz, $CDCl_3$) δ 175.15, 175.1, 157.4, 152.3, 152.3, 148.4, 130.9, 126.2, 125.7, 121.51, 121.5, 118.1, 117.7, 112.5, 102.8, 84.44, 81.4, 84.4, 75.9, 71.8, 68.2, 67.3, 67.27, 41.8, 24.4, 24.3, 20.7, 20.6, 11.5, 11.4.

One-Pot Synthesis of Remdesivir 1 in a 10.0 g Scale. In a flame-dried round-bottom flask, a mixture of the 5-alcohol **7** (10 g, 30.2 mmol) and catalyst **29** (1.8 g, 6.2 mmol) were coevaporated with anhydrous toluene (100 mL, 2 times) and dried under high-vacuum for 2 h. The mixture was dissolved in anhydrous CH_2Cl_2 (500 mL) under N_2 atmosphere, and freshly activated 4 Å molecular sieves (15 g) and 2,6-luditine (7.0 mL, 60.4 mmol) were sequentially added to the solution. The reaction mixture was stirred at room temperature for 10 min, and then cooled to −20 °C. After 10 min, a solution of the phosphoramidoyl chloridates **4** (15.7 g, 45.2 mmol) in anhydrous CH_2Cl_2 (5 mL) was added, and the reaction mixture was stirred at the same temperature for 24 h. Dichloromethane was then evaporated through the needle under reduced pressure. The crude material was treated with p-TSA (57.4 g, 0.3 mol) in methanol (500 mL), and the resulting solution was continuously stirred at room temperature for 24 h. The reaction mixture was filtered through a pad of Celite to remove 4 Å molecular sieves, quenched by adding triethylamine, and concentrated in vacuo. The crude residue was dissolved in EtOAc, and the mixture was washed with saturated $NaHCO_3$. The aqueous layer was extracted with EtOAc (3 × 250 mL), and the combined organic layers were dried over $MgSO_4$, filtered and concentrated in vacuo. The crude residue was subjected to silica gel column chromatography by using EtOAc/hexane (1/9→ 1/1 → 3/1 → 1/0) to afford the catalyst **29** (1.5 g, 83%) and a mixture of the diastereomers, which was further purified by recrystallization from CH_3CN and CH_2Cl_2 to afford remdesivir **1** (13.3 g, 70% yield, 99.3/0.7 d.r.) as a white solid.

■ ASSOCIATED CONTENT

Supporting Information

The Supporting Information is available free of charge at https://pubs.acs.org/doi/10.1021/acs.joc.0c02888.

Copies of ^1H, ^{13}C, and 2D NMR spectra of all new compounds (PDF)

Accession Codes

CCDC 2017880 contains the supplementary crystallographic data for this paper. These data can be obtained free of charge via www.ccdc.cam.ac.uk/data_request/cif, or by emailing data_request@ccdc.cam.ac.uk, or by contacting The Cambridge Crystallographic Data Centre, 12 Union Road, Cambridge CB2 1EZ, UK; fax: +44 1223 336033.

■ AUTHOR INFORMATION

Corresponding Authors

Chi-Huey Wong − *Genomics Research Center, Academia Sinica, Taipei 11529, Taiwan; The Scripps Research Institute, La Jolla, California 92037, United States;* orcid.org/0000-0002-9961-7865; Email: chwong@gate.sinica.edu.tw, wong@scripps.edu

Shang-Cheng Hung − *Genomics Research Center, Academia Sinica, Taipei 11529, Taiwan; Department of Applied Science, National Taitung University, Taitung 95092, Taiwan;* orcid.org/0000-0002-8797-729X; Email: schung@gate.sinica.edu.tw

Authors

Veeranjaneyulu Gannedi − *Genomics Research Center, Academia Sinica, Taipei 11529, Taiwan*

Bharath Kumar Villuri − *Genomics Research Center, Academia Sinica, Taipei 11529, Taiwan*

Sivakumar N. Reddy − *Genomics Research Center, Academia Sinica, Taipei 11529, Taiwan*

Chiao-Chu Ku − *Genomics Research Center, Academia Sinica, Taipei 11529, Taiwan*

Complete contact information is available at: https://pubs.acs.org/10.1021/acs.joc.0c02888

Notes

The authors declare no competing financial interest.

■ ACKNOWLEDGMENTS

This work was supported by the Ministry of Science and Technology of Taiwan (MOST 108-2639-M-001-001-ASP), and the Academia Sinica (AS-KPQ-109-BioMed and AS-SUMMIT-109).

■ REFERENCES

(1) Gorbalenya, A. E.; Baker, S. C.; Baric, R. S.; de Groot, R. J.; Drosten, C.; Gulyaeva, A. A.; Haagmans, B. L.; Lauber, C.; Leontovich, A. M.; Neuman, B. W.; Penzar, D.; Perlman, S.; Poon, L. L. M.; Samborskiy, D. V.; Sidorov, I. A.; Sola, I.; Ziebuhr, J. The species severe acute respiratory syndrome-related coronavirus: classifying 2019-nCoV and naming it SARS-CoV-2. *Nat. Microbiol.* **2020**, *5*, 536−544.

(2) Kupferschmidt, K.; Cohen, J. Will novel virus go pandemic or be contained? *Science* **2020**, *367*, 610−611.

(3) Habibzadeh, P.; Stoneman, E. K. The novel coronavirus: a bird's eye view. *Int. J. Occup. Environ. Med.* **2020**, *11*, 65−71.

(4) Masters, P. S. In Advances in Virus Research. *Adv. Virus Res.* **2006**, *66*, 193−232.

(5) Malik, Y. A. Properties of Coronavirus and SARS-CoV-2. *Malays. J. Pathol.* **2020**, *42*, 3−11.

(6) Letko, M.; Marzi, A.; Munster, V. Functional assessment of cell entry and receptor usage for SARS-CoV-2 and other lineage B betacoronaviruses. *Nat. Microbiol* **2020**, *5*, 562−569.

(7) Hoffmann, M.; Kleine-Weber, H.; Schroeder, S.; Krüger, N.; Herrler, T.; Erichsen, S.; Schiergens, T. S.; Herrler, G.; Wu, N.-H.; Nitsche, A.; Müller, M. A.; Drosten, C.; Pöhlmann, S. SARS-CoV-2 cell entry depends on ACE2 and TMPRSS2 and is blocked by a clinically proven protease inhibitor. *Cell* **2020**, *181*, 271−280.

(8) Zhang, H.; Penninger, J. M.; Li, Y.; Zhong, N.; Slutsky, A. S. Angiotensin-converting enzyme 2 (ACE2) as a SARS-CoV-2 receptor: molecular mechanisms and potential therapeutic target. *Intensive Care Med.* **2020**, *46*, 586−590.

(9) Yan, R.; Zhang, Y.; Li, Y.; Xia, L.; Guo, Y.; Zhou, Q. Structural basis for the recognition of SARS-CoV-2 by full-length human ACE2. *Science* **2020**, *367*, 1444−1448.

(10) Tang, T.; Bidon, M.; Jaimes, J. A.; Whittaker, G. R.; Daniel, S. Coronavirus membrane fusion mechanism offers a potential target for antiviral development. *Antiviral Res.* **2020**, *178*, 104792−104808.

(11) Sharma, A.; Gupta, S. P. In *Viral Proteases and Their Inhibitors*; Gupta, S. P., Ed.; Academic Press, 2017; pp 1−24.

(12) Aftab, S. O.; Ghouri, M. Z.; Masood, M. U.; Haider, Z.; Khan, Z.; Ahmad, A.; Munawar, N. Analysis of SARS-CoV-2 RNA-dependent RNA polymerase as a potential therapeutic drug target using a computational approach. *J. Transl. Med.* **2020**, *18*, 275−290.

(13) Fehr, A. R.; Perlman, S. Coronaviruses: an overview of their replication and pathogenesis. *Methods Mol. Biol.* **2015**, *1282*, 1−23.

(14) Ruch, T. R.; Machamer, C. E. The coronavirus E protein: assembly and beyond. *Viruses* **2012**, *4*, 363−382.

(15) Eastman, R. T.; Roth, J. S.; Brimacombe, K. R.; Simeonov, A.; Shen, M.; Patnaik, S.; Hall, M. D. Remdesivir: A review of its discovery and development leading to emergency use authorization for treatment of COVID-19. *ACS Cent. Sci.* **2020**, *6*, 672−683.

(16) Warren, T. K.; Jordan, R.; Lo, M. K.; Ray, A. S.; Mackman, R. L.; Soloveva, V.; Siegel, D.; Perron, M.; Bannister, R.; Hui, H. C.; Larson, N.; Strickley, R.; Wells, J.; Stuthman, K. S.; Van Tongeren, S.

A.; Garza, N. L.; Donnelly, G.; Shurtleff, A. C.; Retterer, C. J.; Gharaibeh, D.; Zamani, R.; Kenny, T.; Eaton, B. P.; Grimes, E.; Welch, L. S.; Gomba, L.; Wilhelmsen, C. L.; Nichols, D. K.; Nuss, J. E.; Nagle, E. R.; Kugelman, J. R.; Palacios, G.; Doerffler, E.; Neville, S.; Carra, E.; Clarke, M. O.; Zhang, L.; Lew, W.; Ross, B.; Wang, Q.; Chun, K.; Wolfe, L.; Babusis, D.; Park, Y.; Stray, K. M.; Trancheva, I.; Feng, J. Y.; Barauskas, O.; Xu, Y.; Wong, P.; Braun, M. R.; Flint, M.; McMullan, L. K.; Chen, S. S.; Fearns, R.; Swaminathan, S.; Mayers, D. L.; Spiropoulou, C. F.; Lee, W. A.; Nichol, S. T.; Cihlar, T.; Bavari, S. Therapeutic efficacy of the small molecule GS-5734 against Ebola virus in rhesus monkeys. *Nature* **2016**, *531*, 381−385.

(17) Siegel, D.; Hui, H. C.; Doerffler, E.; Clarke, M. O.; Chun, K.; Zhang, L.; Neville, S.; Carra, E.; Lew, W.; Ross, B.; Wang, Q.; Wolfe, L.; Jordan, R.; Soloveva, V.; Knox, J.; Perry, J.; Perron, M.; Stray, K. M.; Barauskas, O.; Feng, J. Y.; Xu, Y.; Lee, G.; Rheingold, A. L.; Ray, A. S.; Bannister, R.; Strickley, R.; Swaminathan, S.; Lee, W. A.; Bavari, S.; Cihlar, T.; Lo, M. K.; Warren, T. K.; Mackman, R. L. Discovery and synthesis of a phosphoramidate prodrug of a pyrrolo[2,1-f][triazin-4-amino] adenine C-nucleoside (GS-5734) for the treatment of Ebola and emerging viruses. *J. Med. Chem.* **2017**, *60*, 1648−1661.

(18) Mulangu, S.; Dodd, L. E.; Davey, R. T.; Tshiani Mbaya, O.; Proschan, M.; Mukadi, D.; Lusakibanza Manzo, M.; Nzolo, D.; Tshomba Oloma, A.; Ibanda, A.; Ali, R.; Coulibaly, S.; Levine, A. C.; Grais, R.; Diaz, J.; Lane, H. C.; Muyembe-Tamfum, J.-J. A randomized, controlled trial of Ebola virus disease therapeutics. *N. Engl. J. Med.* **2019**, *381*, 2293−2303.

(19) Wang, M.; Cao, R.; Zhang, L.; Yang, X.; Liu, J.; Xu, M.; Shi, Z.; Hu, Z.; Zhong, W.; Xiao, G. Remdesivir and chloroquine effectively inhibit the recently emerged novel coronavirus (2019-nCoV) in vitro. *Cell Res.* **2020**, *30*, 269−271.

(20) de Wit, E.; Feldmann, F.; Cronin, J.; Jordan, R.; Okumura, A.; Thomas, T.; Scott, D.; Cihlar, T.; Feldmann, H. Prophylactic and therapeutic remdesivir (GS-5734) treatment in the rhesus macaque model of MERS-CoV infection. *Proc. Natl. Acad. Sci. U. S. A.* **2020**, *117*, 6771−6776.

(21) Cho, A.; Saunders, O. L.; Butler, T.; Zhang, L.; Xu, J.; Vela, J. E.; Feng, J. Y.; Ray, A. S.; Kim, C. U. Synthesis and antiviral activity of a series of 1′-substituted 4-aza-7,9-dideazaadenosine C-nucleosides. *Bioorg. Med. Chem. Lett.* **2012**, *22*, 2705−2707.

(22) Thornton, P. J.; Kadri, H.; Miccoli, A.; Mehellou, Y. Nucleoside phosphate and phosphonate prodrug clinical candidates. *J. Med. Chem.* **2016**, *59*, 10400−10410.

(23) Ghosh, A.; Shieh, J. J.; Pan, C. J.; Sun, M. S.; Chou, J. Y. The catalytic center of glucose-6-phosphatase. HIS176 is the nucleophile forming the phosphohistidine-enzyme intermediate during catalysis. *J. Biol. Chem.* **2002**, *277*, 32837−32842.

(24) Liu, S.; Zhang, Z.; Xie, F.; Butt, A. N.; Sun, L.; Zhang. First catalytic enantioselective synthesis of *P*-stereogenic phosphoramides via kinetic resolution promoted by a chiral bicyclic imidazole nucleophilic catalyst. *Tetrahedron: Asymmetry* **2012**, *23*, 329−332.

(25) De Miranda, A.; Gomes, J. C.; Rodrigues, M. T., Jr.; Costa, I. C. R.; Almeida, W. P.; Lopes, R.; Miranda, L. S. M.; Coelho, F.; de Souza, R. O. M. A. Kinetic resolution of 5*H*-pyrrolo[1,2-*a*]imidazol-7-ol, 6,7-dihydro under continuous flow conditions: An intermediate for chiral ionic liquids synthesis. *J. Mol. Catal. B: Enzym.* **2013**, *91*, 77−80.

(26) DiRocco, D. A.; Ji, Y.; Sherer, E. C.; Klapars, A.; Reibarkh, M.; Dropinski, J.; Mathew, R.; Maligres, P.; Hyde, A. M.; Limanto, J.; Brunskill, A.; Ruck, R. T.; Campeau, L.-C.; Davies, I. W. A multifunctional catalyst that stereoselectively assembles prodrugs. *Science* **2017**, *356*, 426−430.

(27) Wang, M.; Zhang, L.; Huo, X.; Zhang, Z.; Yuan, Q.; Li, P.; Chen, J.; Zou, Y.; Wu, Z.; Zhang, W. Catalytic asymmetric synthesis of the anti-COVID-19 drug remdesivir. *Angew. Chem., Int. Ed.* **2020**, DOI: 10.1002/anie.202011527.

(28) Zhang, Z.; Xie, F.; Jia, J.; Zhang, W. Chiral Bicycle Imidazole Nucleophilic Catalysts: Rational Design, Facile Synthesis, and Successful Application in Asymmetric Steglich Rearrangement. *J. Am. Chem. Soc.* **2010**, *132*, 15939−15941.

(29) Chun, B. K.; Clarke, M. H.; Doerffler, E.; Hui, H. C.; Jordan, R.; Mackman, R. L.; Parrish, J. P.; Ray, A. S.; Siegel, D. Methods for treating filoviridae virus infections. WO2016/69826, 2016, A1.

https://dx.doi.org/10.1021/acs.joc.0c02888
J. Org. Chem. 2021, 86, 4977−4985